Petroleum and Coal

**Article** **Open Access**

# Characterization of Bara Formation coals in Lakhra region, Lower Indus Basin Pakistan: Implication of hydrocarbon generation potential and depositional environment

*Zain Gul[1], Wan Hasiah Abdullah[2], Yousif M. Makeen Ahmed[3], Muhammad Jamil[1], Nisar Ahmed[1]*

[1] *Department of Geoscience, Universiti Teknologi PETRONAS. 32610 Seri Iskandar, Perak, Malaysia*
[2] *Department of Geology, University of Malaya, Malaysia*
[3] *College of Earth Science, Jilin University, Changchun, China*

Received June 26, 2020; Accepted October 15, 2020

**Abstract**

To date, very little has been published on the organic geochemical and petrological aspects of the Bara formation coals, Southern Indus Basin, Pakistan. To address this, fresh unweathered coal samples were collected from seven different coal mines of the Lakhra coal field and were subsequently analysed and evaluated in detail. Numerous characteristics were assessed i.e. thermal maturity (coal rank), petroleum generation potential, type of organic matter and paleo-depositional environment. Evaluation techniques include proximate analysis, bitumen (soluble organic matter) extraction, fractionation of hydrocarbon yield using liquid column chromatography, Rock Eval, pyrolysis-GC (Py-GC), GC-MS, huminite/vitrinite reflectance and maceral analysis. Based on proximate analysis, the samples are classified as lignite to subbituminous C based on the ASTM standard. This low rank is supported by extracted bitumen and Rock Eval data. Although immature, these Lakhra coals show to possess excellent hydrocarbon generation potential. The distributions of n-alkanes, isoprenoid, hopane and sterane biomarkers further corroborate that these coals are thermally immature for hydrocarbon generation. The probable paleodepositional environment interpreted based on biomarkers and maceral analysis data suggests a waterlogged swamp in a lower delta plain setting that experienced frequent marine influence as indicated by the sub-oxic condition of deposition.

***Keywords***: *Bara Formation Coal; Organic geochemistry; Coal petrology; Thermal maturity; Kerogen type II/III; Paleo-depositional setting; Biomarkers.*

## 1. Introduction

Coal resources has always been in consideration for transport, industry utilization and for other miscellaneous purposes [1-3]. Moreover, due to its organic rich nature its thoroughly been studied for hydrocarbon potential purposes [4-7] and proven that it can be a possible source rock in petroleum system. Thus, Bara Formation consist of large coal reserves and its regionally wide spreads [8-11], due to limited outcrop exposure on the surface, the samples has been collected from underground mines operated by Lakhra Coal Development Company (LCDC) located in small town named Khanote, District Jamshoro and almost 40 km south east to Hyderabad District, Sindh Pakistan Fig. 1C. Based on [10] investigation coal indicates good permeability characterized as subbituminous C to lignite A. Whilst, cleat and fracture investigation good permeability for CBM storage [12]. To date, limited studies has been recorded which established detail hydrocarbon source rock profile. Therefore, in this study we have incorporated organic geochemical and organic petrological analyses in order to assess coal quality, thermal maturity/rank, hydrocarbon generation potential and the paleo depositional condition of Bara Formation coal. This integration of methods is commonly performed in such studies as conducted by previous workers [13-16]. In this current study, the derived data and parameters that were gathered include volatile, moisture, ash, carbon, Rock-Eval pyrolysis data and total organic content (TOC), Kerogen (Py-GC), vitrinite/huminite reflectance (%$R_o$) and maceral analysis. Moreover, bitumen extraction and biomarker data were used as supporting evidence for assessment of thermal maturity and depositional environment of the analysed Bara Formation coals.

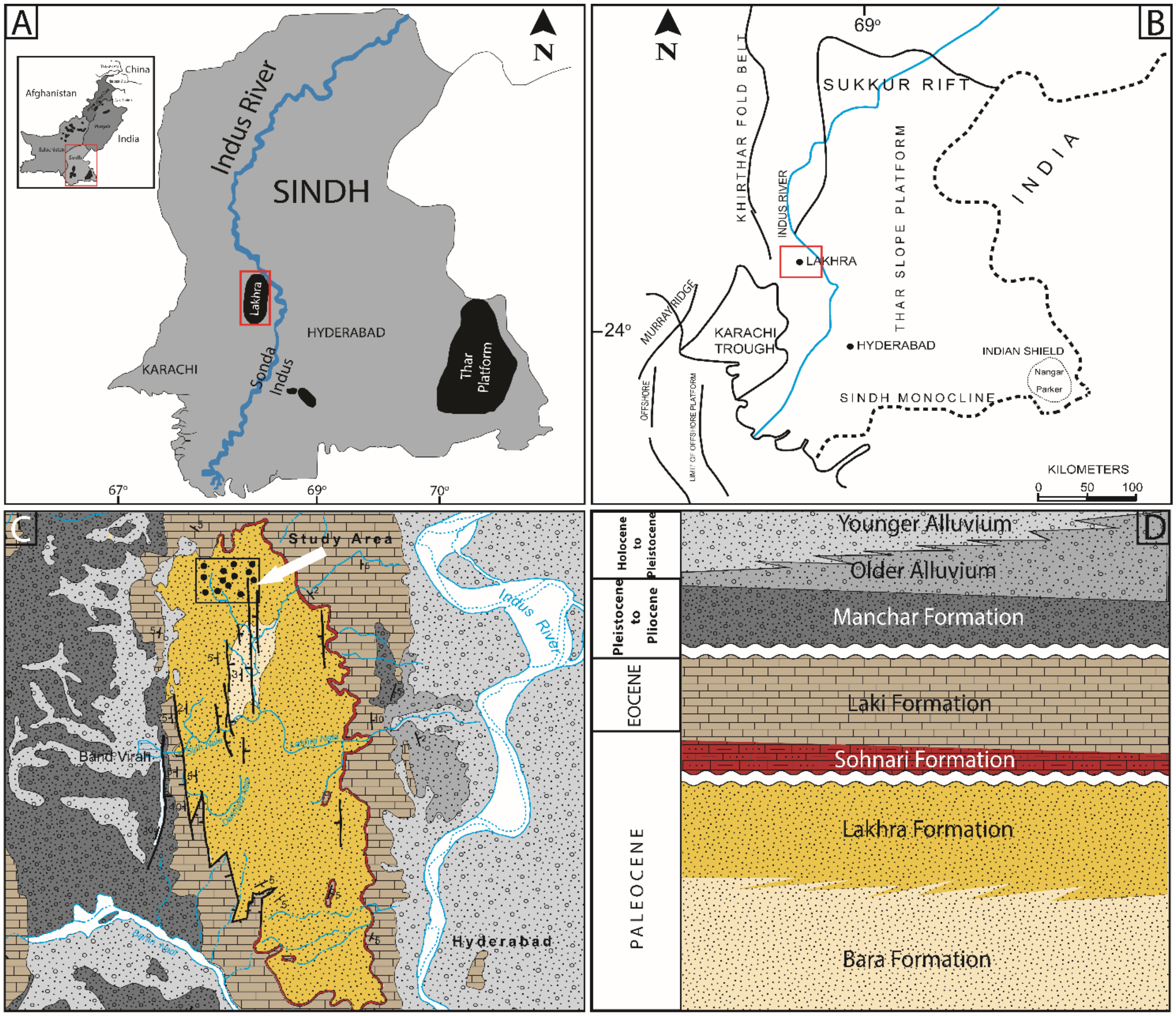

Figure 1. (A) showing location map of the study area, (B) showing structural setting of the southern Indus Basin (modified after [12]). (C) Showing stratigraphic distribution of Lakhra region (modified after [13] and [14]). (D) showing the stratigraphic column of Tertiary sediments of the lower Indus basin within the study area (*modified after [15]*).

## 2. Geological settings

The Indus Basin is divided into three parts: Lower/southern Indus Basin, Middle Indus Basin and Upper Indus Basin. Lower Indus basin spreads almost 150,000 square miles with 38,000 ft of vertical sequences composed of Jurassic, cretaceous and tertiary sediments [2,8].

The Lower Indus basin is structurally bounded by Sukkur Rift (Jacobabad-Kandhkot high) in the north. Indian shield in the east (Nangar Parker) and marginal zone (Indian Plate) in the west Fig. 1B. The stratigraphic sequence consists of the rocks from Precambrian to recent age that are mainly dominated by Jurassic, Cretaceous, and Tertiary sediments. In this study, our focus is on Tertiary formations; from top to bottom are Laki, Sonhari, Lakhra and Bara Formation respectively Fig. 1D. The Bara Formation is composed of siliciclastic sediments mainly of claystone, shale, siltstone and having multiple coal seams [19]. The Lakhra Formation rocks shows similar characteristics to Bara Formation, the only difference is noted is the presence of limestone. Thus, it predominantly consists siliciclastic sediments, initiated with sandstone bed at the base and top part is dominated by limestone often appears as interbedded with siliciclastic materials [10-11].

Lakhra formation is covered widespread sitting at the top of Bara Formation and unconformably overlies the upper Laki limestone. In some parts, Laki limestone is eroded due to post-Ranikot erosion [19] only leaving place to Manchar Formation sitting at the top of Ranikot group formations. Nuttall [21] subdivided the [22]"Laki Series" into 2 units, of which the lower unit, a lateritic claystone, he named the Basal Laki laterite or Sonhari formation, and the upper unit Laki limestone. In outcrops the "Basal Laki laterite" is a highly ferruginous, dark red, maroon, dark brown, and yellowish-brown massive claystone containing concretions of iron oxide, Locally, where the overlying limestone has been stripped off by erosion, the laterite has a duricrust or hardpan on exposed surfaces. On the surface the "Basal Laki laterite" is a widespread, very conspicuous lithologic unit in the Lakhra area; even partially exposed outcrops are readily recognizable when viewed in the field from great distances.

No diagnostic fossils have been found in rocks of the "Basal Laki laterite" by which to ascertain its age. Since the laterite is regarded to be the lowermost unit of the Laki Limestone, it is considered early Eocene (Ypresian) in age [21-22]. The Laki Limestone is equivalent to the "Laki Series" of Verdenburg [22] who derived the term from the Laki hill range and village in the western part of the Hyderabad. The formation consists of finely crystalline limestone and very subordinate amounts of claystone or marl. The limestone is light yellowish-gray, white, and light gray, stained yellow to brown, and weathers to light gray. It is a nodular, hard, resistant, massive, and commonly forms cliff. Foraminifera abounds throughout the formation, but most of the megafauna is present in the middle part. [23-24] considered the "Laki Series" to be early Lutetian in age. Later work by [21] shows that the "Laki Series" corresponds to the Ypresian. The youngest rocks in the area are unconsolidated stream, colluvial, and eolian deposits composed of sandstone, siltstone, claystone, and limestone and sandstone pebble and cobble beds. The alluvium is as much as 10 feet thick or more in places and is widespread in the western part. Stream-laid deposits are present in the larger watercourses in the central and eastern parts [19].

## 3. Sample and methods

A total of seven coal samples were collected from the Bara Formation from seven different coal mines, 2 from block A and 5 from block B of Lakhra coal field, these samples are labeled as per mined identification. The coal is currently been extracted for industry utilization purpose.

The quality of a Lakhra coal was previously studied using the ASTM (American society of testing materials) method [10]. In this current study, the ASTM analysis was performed on all of the seven investigated coal samples. The coal quality of these coals was also analyzed using a thermogravimetric Analyzer (TGA) DTA/DSC TA (Model SDT Q600) on crushed samples to determine fixed carbon, volatile matter, moisture and ash content.

Rock-Eval 6 together with TOC component were performed on crushed samples for pyrolysis analysis. The measured parameter includes, TOC (Total organic carbon), $T_{max}$ (temperature of maximum pyrolysis yield), $S_1$ (volatile hydrocarbon content, mg HC/g rock), $S_2$ (remaining Hydrocarbon generating potential) and $S_3$ (carbon dioxide yield, mg $CO_2$/g rock). OI (oxygen index), PI (production index) and HI (hydrogen index) were calculated as suggested by [24].

Approximately 2g of the crushed powdered samples were extracted using Soxhlet apparatus with (93:7) dichloromethane and methanol ($CH_3OH$) mixture for 72 hours. The extracted organic matter (EOM), also referred to as bitumen, were further fractioned into saturated, aromatic and polar fractions using liquid column chromatography and were developed with petroleum ether, dichloromethane and methanol respectively. For analysis of biomarker distributions, gas chromatography (GC) were performed on saturated fractions using an Agilent 6890N series GC. Aliphatic fractions were dissolved in hexane and analyzed in a GC with a HP-5MS column, and temperate held at 30 min at 300°C. Gas chromatography-mass spectrometry (GC-MS) analysis was carried on a V 5975B inert MSD mass spectrometer together with gas chromatograph and an attached ion source (70 eV ionization, 230°C interface temperature, 100 mA filament emission current). The acquired fingerprints from the GC and GCMS were interpreted for biomarker identification. Pyrolysis gas chromatography (Py-GC) using Frontier Lab Pyrolyser and pyrolysis (at 600°C) were applied on crushed samples to identify kerogen types as described by previous workers [25-26].

Organic petrographic examination including vitrinite reflectance measurement and maceral microscopy were performed on polished block in order to established thermal maturity and maceral content. The analysis was carried out at organic petrographic laboratories of the Department of Geology at University of Malaya. The polished block was prepared by mounting whole rock fragments, using slow setting polyster resin (serfix) mixed with resin hardener and set to dry. The mounted samples were ground flat on diamond lap, using water as lubricant and subsequently polished using silicon carbide paper (P800, P2400 and P4000) grades. Samples were finally polished for highly reflecting surface using finer alumina suspension (1 µm, 0.3 µm and 0.5 µm).

Petrographic analysis was conducted on a LEICA DM6000M microscope and LEICA CTR6000 photometry system equipped with fluorescence illuminators under plane polarized reflected light. Filter system used for analysis are LP425 suspension filter, BP 340-380 excitation filters and RKP 400 dichromatic mirror.

Maceral composition has been identified by counting 1000 points under UV (ultraviolet) and reflected white "light". Vitrinite/huminite reflectance was measured under oil immersion (%Ro) by using DISKUS fossil/Maceral software package.

## 4. Results

### 4.1. Proximate analysis and coal rank

The results of the proximate analysis performed in this study shown in Table 1 indicate that the coals are thermally immature based on the fixed carbon contents and volatile matter in the range of 26.17-47.32 and 35.44-53.07 wt% respectively. The measurement of huminite/vitrinite reflectance (%Ro) seems to concur with this interpretation, whereby the %Ro values varies between 0.26 and 0.36%. This is in agreement with values of volatile matter and fixed carbon contents based on ASTM method which indicates that these coals are of sub-bituminous C to Lignite rank.

Table 1. TGA results performed in this study and compared to a previous study based on ASTM method

| Analysis | ASTM | Thermogravimetric analyzer | | | | | | |
|---|---|---|---|---|---|---|---|---|
| | | LCDC A21 | LCDC A33 | LCDC B4A | LCDC B27 | LCDC B31 | LCDC B63 | LCDC B39 |
| Moisture % | 28 | 6.41 | 8.97 | 2.62 | 3.36 | 2.39 | 28.74 | 11.34 |
| Volatile matter % | 28 | 51.05 | 53.07 | 45.64 | 52.06 | 35.44 | 39.65 | 43.48 |
| Ash % | 15 | 0.24 | 0.13 | 0.09 | 0.18 | 9.60 | 0.11 | 0.03 |
| Carbon % | 39 | 37.66 | 37.18 | 47.32 | 40.61 | 26.17 | 28.20 | 32.03 |

### 4.2. Bitumen extraction: Extractable organic matter (EOM) data

The results from bitumen extraction process were gathered and tabulated. The amount of EOM ranges from 10,528 ppm to 27,453 ppm. Generally, if amount of EOM is greater than 5,000 ppm, it is considered as having a very good hydrocarbon generation potential based on classification by [27]). The concentrations of the EOM are shown in Table 2 and Fig. 2b. The EOM were further fractioned into aliphatic, aromatic and polar compounds Fig. 2a. The recovered aliphatic fractions ranges from 820 to 2,884 ppm with yield of 5.29% to 14.36% for EOM, while aromatic hydrocarbon recovered ranges from 2,869 ppm to 9,272 ppm with yield of 23.56% to 44.31%. The collected NSO compounds were around 5,291 ppm to 17,323 ppm with yield of 50.52% to 62.06%. Fractions from bitumen indicates that the NSO compounds are more dominant then saturated and aromatic, while aromatic hydrocarbons are more dominant compared to saturated hydrocarbon. Previous studies e.g.[21-22,25-26] reported that the abundance of NSO compounds are more common in coal, whereas the dominance of aromatic over saturated hydrocarbon indicates that the samples are gas-prone or having mixed oil and gas potential.

Table 2. Bitumen extraction and liquid column chromatography data (in ppm)

| Coal Field | Sample ID | Bitumen Extraction and chromatographic fraction (ppm of whole rock) | | | | | Chromatographic fractions of Bitumen Extraction (EOM wt %) | | | |
|---|---|---|---|---|---|---|---|---|---|---|
| | | EOM | SAT | ARO | NSO | HC | Sat | Aro | NSO | HC |
| Lakhra coal field | LCDC A21 | 17240 | 1814 | 6715 | 8711 | 5829 | 10.52 | 38.95 | 50.52 | 49.47 |
| | LCDC A33 | 27453 | 1454 | 9272 | 16727 | 10726 | 5.29 | 33.77 | 60.92 | 39.07 |
| | LCDC B4A | 14425 | 819 | 6393 | 7213 | 7212 | 5.68 | 44.31 | 50.00 | 49.99 |
| | LCDC B27 | 28115 | 1529 | 9263 | 17323 | 10765 | 5.43 | 32.94 | 61.61 | 38.37 |
| | LCDC B31 | 10528 | 1005 | 4232 | 5291 | 5237 | 9.54 | 40.19 | 50.25 | 49.74 |
| | LCDC B63 | 12167 | 1748 | 2867 | 7552 | 4615 | 14.36 | 23.56 | 62.06 | 37.93 |
| | LCDC B39 | 22883 | 2884 | 6346 | 13653 | 9230 | 12.60 | 27.73 | 59.66 | 40.33 |

*HC = Hydrocarbon fractions (Saturated + Aromatic); NSO = Nitrogen, Sulphur, Oxygen components;*
*Aro= Aromatic hydrocarbons; Sat = Saturated hydrocarbons;*
*EOM = Extractable organic matter (Bitumen extraction).*

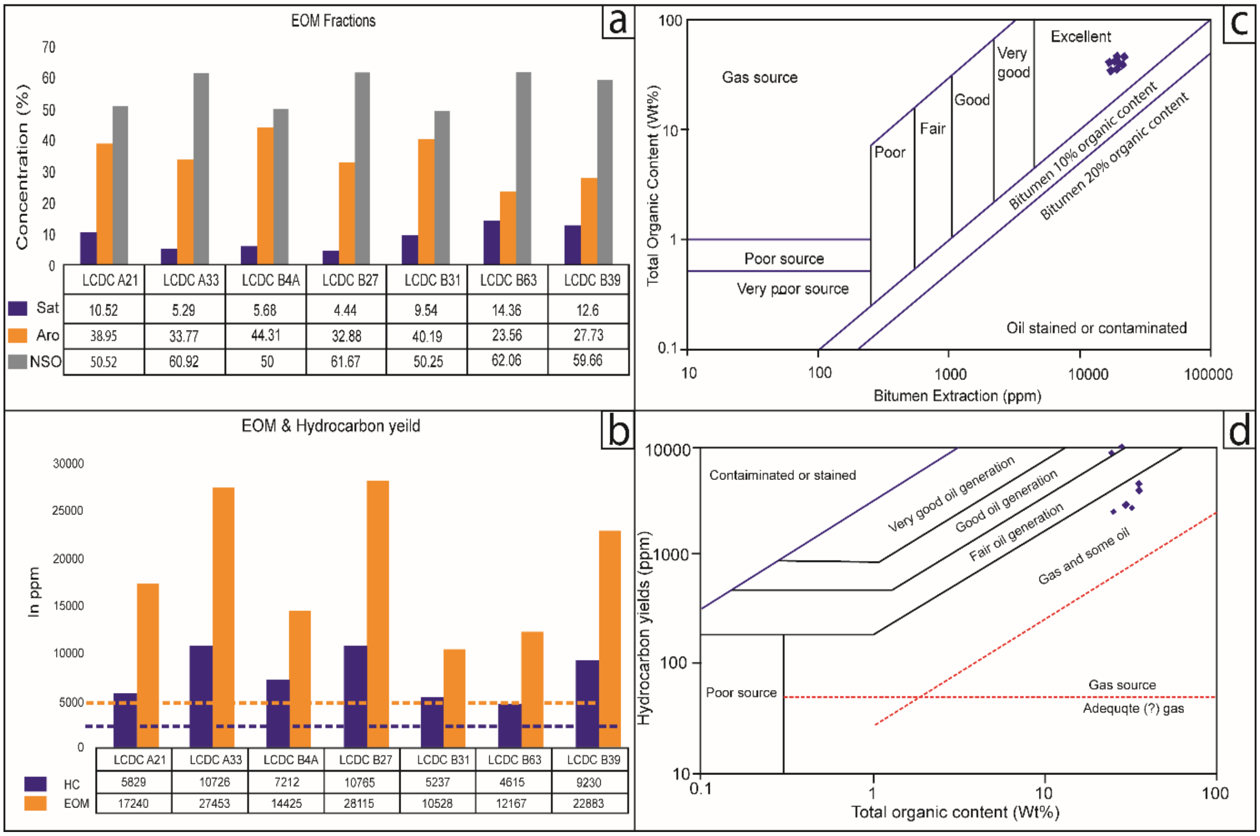

Figure 2. (a) Histogram of fractions concentration from bitumen extraction data, (b) Histogram indicates the amount of extracted Hydrocarbon yield and EOM; lines indicate it has excellent generation potential if exceeds. (c) Hydrocarbon yield versus TOC indicates about quality of the samples (modified after [26]) and (d), TOC versus bitumen (ppm) indicates the generating potential

The combination of saturated hydrocarbon and aromatic hydrocarbons is referred to as hydrocarbon fraction. The amount of hydrocarbon recovered ranges from 4,615 to 10,726 ppm representing yield of 37% to 49% which indicates that the samples possess excellent hydrocarbon generation potentials Fig. 2a. The hydrocarbon generating potential data of the analysed Bara Formation coals were presented in modified plots used by [29] together with classification of [27] Fig. 2 c & d. The plots show that the studied coal samples possess viable source rocks potential with predominantly excellent gas and fairly good oil generation capability.

### 4.3. Rock Eval 6 and pyrolysis analysis

Rock-Eval pyrolysis and TOC analysis were performed with the purpose to identify the petroleum generation potential, quality and type of organic matter as well as the thermal maturity of the studied samples. As expected for coals, high TOC values were obtained that ranges from 37.89 to 62.75 wt% and is considered to possess excellent petroleum generation potential. Meanwhile, the parameter $S_2$ that represents free hydrocarbons generated during pyrolysis range from 93.52 to 243.84 which is also useful to evaluate the generation potential of source rocks [25,27-28]. The parameter $S_1$ represents the volatile hydrocarbon ranging from 1.68 – 5.39 which also indicate excellent hydrocarbon generation potential. $S_3$ represents the amount of carbon dioxide present in samples. It is also useful in interpreting the coal quality. In addition, $T_{max}$ value which represents the temperature at the point where S2 peak is at maximum is also determined. The $T_{max}$ values range from 403-429$^{o}$C thus indicating organic matter is thermally immature for hydrocarbon generation. Hydrogen index (HI) and oxygen index (OI) of the studied samples were calculated and determined to be in the range of 375-213 mg HC/g TOC and 0-20 mg $CO_2$/g TOC, respectively Table 3. A diagram of Fig. 3 a & b was based of pyrolysis data, kerogen classification and thermal maturity using the HI versus $T_{max}$ and HI versus OI data shown that the Lakhra coals are dominated by Type II/III kerogens. In this respect, all the analyzed samples are generally plotted in the immature organic matter region of mixed Type II/III kerogens. Moreover, by plotting S2/S3 versus TOC results and S2 versus TOC on classified diagram of Fig. 3 c & d suggest the analysed coals are of mixed oil and gas-prone characters with excellent remaining hydrocarbon generating potentials.

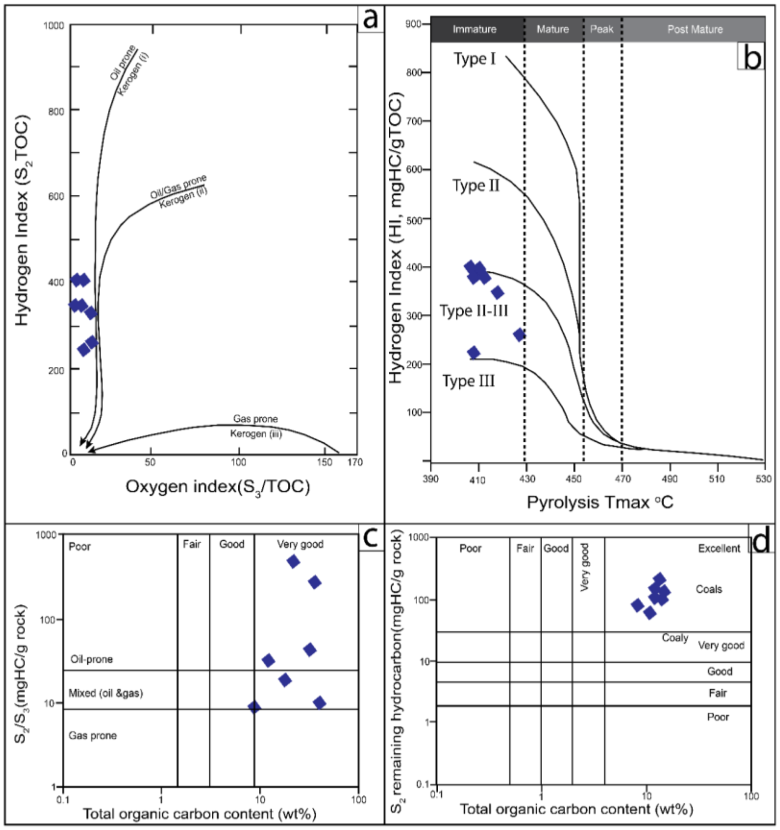

Figure 3. (a) Hydrogen versus oxygen index (OI) indicates kerogen quality, (b) Plot of Hydrogen Index (HI) versus pyrolysis Tmax indicates thermal maturity of the analysed coal samples from Lakhra coal field (c) Plot of total organic carbon S2/S3 versus (TOC) yields showing hydrocarbon generative potential and, (d) Pyrolysis S2 versus total organic carbon (TOC) plot showing generative source rock potential from coal from Lakhra coal field of the studied coals modified after [26].

Table 3. Results of TOC and Rock Eval pyrolysis analysis with calculated parameters for the Lakhra coal field samples

| Coal field | Sample ID | Lithology | Pyrolysis data | | | | | | | | |
|---|---|---|---|---|---|---|---|---|---|---|---|
| | | | TOC | $S_1$ | $S_2$ | $S_3$ | Tmax | S2/S3 | HI | OI | PI |
| | | | | (mg/g) | (mg/g) | (mg/g) | (°C) | | | | |
| Lakhra coal field | LCDC A21 | Coal | 60.46 | 3.61 | 212.30 | 8 | 417 | 26.53 | 351 | 14 | 0.02 |
| | LCDC A33 | Coal | 53.23 | 3.67 | 199.73 | 0.24 | 404 | 832.2 | 375 | 0 | 0.02 |
| | LCDC B4A | Coal | 62.75 | 3.81 | 159.65 | 10.36 | 429 | 15.41 | 254 | 17 | 0.02 |
| | LCDC B27 | Coal | 60.47 | 5.39 | 243.84 | 0.39 | 410 | 625.2 | 403 | 1 | 0.02 |
| | LCDC B31 | Coal | 37.89 | 3.35 | 156.12 | 4.11 | 407 | 37.98 | 412 | 11 | 0.02 |
| | LCDC B63 | Coal | 53.69 | 3.66 | 200.11 | 2.96 | 404 | 67.60 | 373 | 6 | 0.02 |
| | LCDC B39 | Coal | 43.92 | 1.68 | 93.52 | 8.71 | 403 | 10.73 | 213 | 20 | 0.02 |

*TOC: Total Organic Carbon, wt %.;*
*Tmax: Temperature at maximum of S2 peak;*
*Hydrogen Index= S2 X 100/TOC, mg HC/g;*
*$S_2$: Remaining HC generative potential, mg HC/g rock;*
*PI: Production Index = S1/(S1 + S2);*
*OI: Oxygen Index= S3 X 100/TOC, mg $CO_2$/g TOC;*
*S3: Carbon dioxide yield, mg $Co_2$ /g rock;*
*$S_1$: Volatile Hydrocarbon (HC) content, mg HC/g rock;*

### 4.4. Kerogen pyrolysis (Py-GC)

In addition to Rock-Eval, pyrolysis-GC was performed to verify the kerogen type, because many workers believed that the data from Rock-Eval equipment does not always represent accurate types of hydrocarbon generated from source rocks e.g. [25-26,31-32]. However, it is an additional benefit to have Rock-Eval pyrolysis data as it is commonly used to interpret kerogen types and to some extent, can differentiate the variation between petroleum composition. This characteristic gives a straight forward indication about the hydrocarbon which can be generated from kerogen type during the maturation process [25,33–35].

The Py-GC fingerprints Fig. 4 of the analyzed samples indicate that the studied coal samples possess mixed oil and gas potential as characterized by the dominance of aromatic compounds over n-alkene/alkane doublets. The distributions of these doublets, as expected, concur that the coals are derived from terrestrial sources e.g. [29, 36–39]. The studied samples show that the n-alkane/alkene doublets chains extend beyond $C_{30}$ which indicates that these coals are aliphatic-rich whilst the abundance of aromatic compounds suggesting a mixed kerogen type (oil and gas-prone). In addition, three pyrolystate components (m, p-xylene, phenol and n-octane) were identified Fig. 5 which indicates a mixture of Type II/III [38-39]. Based on this ternary plot, the majority of the analyzed coal samples fall within the Type II/III kerogen. This is in support of their HI values which ranges from 213 to 403 mgHC/TOC, thus indicates a mixed oil and gas generating potential.

### 4.5. GC and GC-MS

#### *4.5.1. Distribution of n-alkanes and isoprenoids*

The gas chromatography (GC) and gas chromatography–mass spectrometry (GC–MS) analyses were performed on the saturated hydrocarbon fraction of the analyzed coal samples Fig. 4. Ion m/z 85 is used to interpret the distribution of n-alkanes and isoprenoids. Parameters derived from ion m/z 85, are commonly applied in organic geochemistry to recognize the paleo-depositional condition and maturity stage of source rock extracts [37,40–43]. The calculated parameters for the analyzed samples are listed in Table 4. The distribution of n-alkanes and isoprenoids show a bimodal distribution. This distribution also shows odd majority of the heavier members (n-C25+) which gave moderate to high CPI values in the range of 1.15–1.41. These CPI values >1 would be expected as the Lakhra coal is immature and predominantly consist of terrestrial derived higher plants [43–45]. Isoprenoids, in particular pristane, occur in high relative abundance, with pristane/phytane (Pr/Ph) ratios >1.0 (1.46–2.41) which suggest that these coals were deposited under suboxic conditions [46–48]. Pristane concentrations are generally lower than the closely eluting n-alkane (n-$C_{17}$) in the analyzed samples see Fig. 5b and Table 5. Meanwhile Pr/n-$C_{17}$ versus Ph/n-$C_{18}$ plot that represent relationship between the kerogen type and depositional environment suggested that the analyzed samples were deposited within a transitional environment, which strongly supports a mixed environment of terrestrial with marine influence as indicated by the bimodal distribution of n-alkanes described earlier.

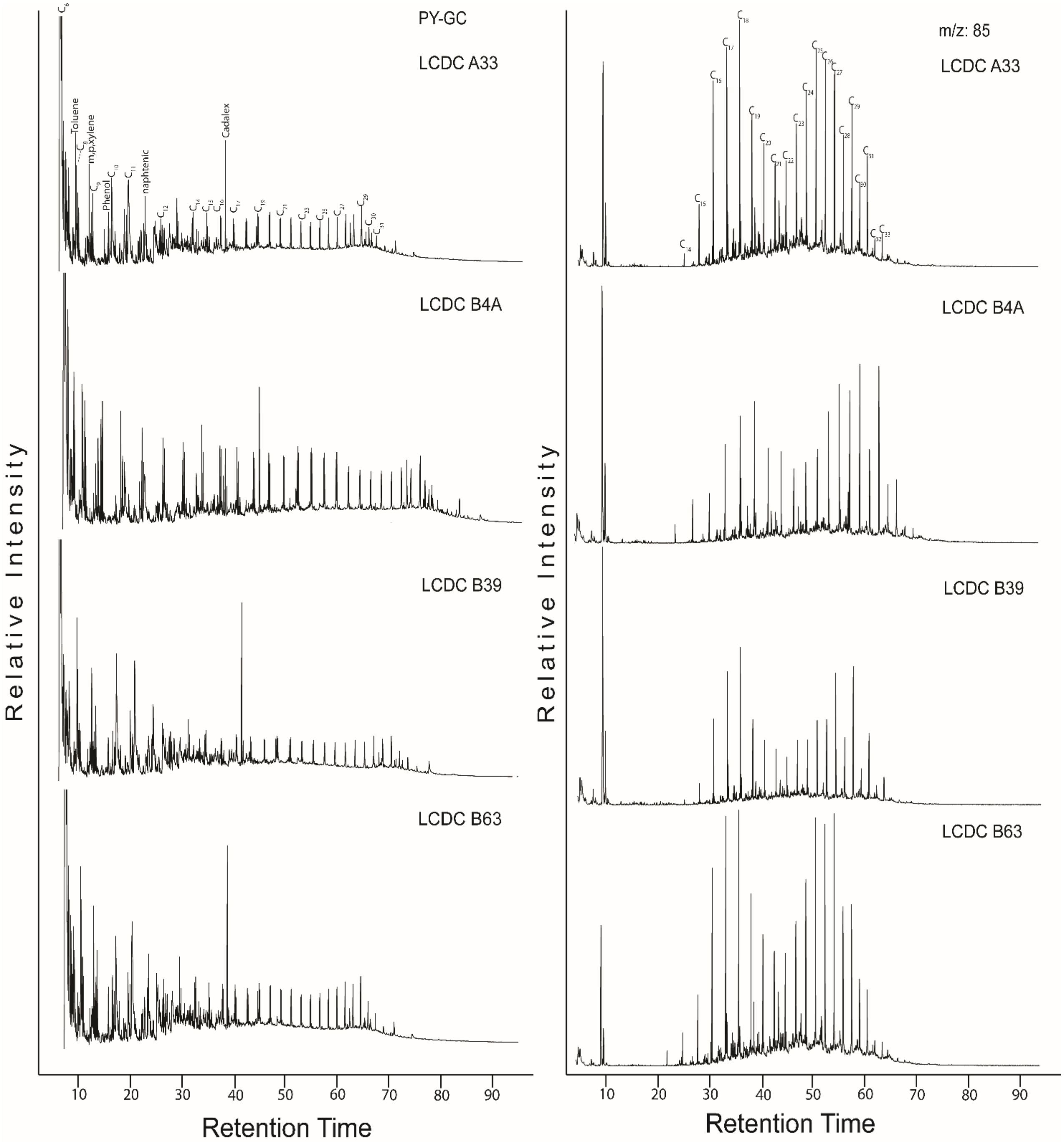

Figure 4. PyGC pyrograms of coal samples LCDC BA33, LCDC B4A, LCDC B39, and LCDC B63 n-alkanes and isopronoids distribution in m/z 85

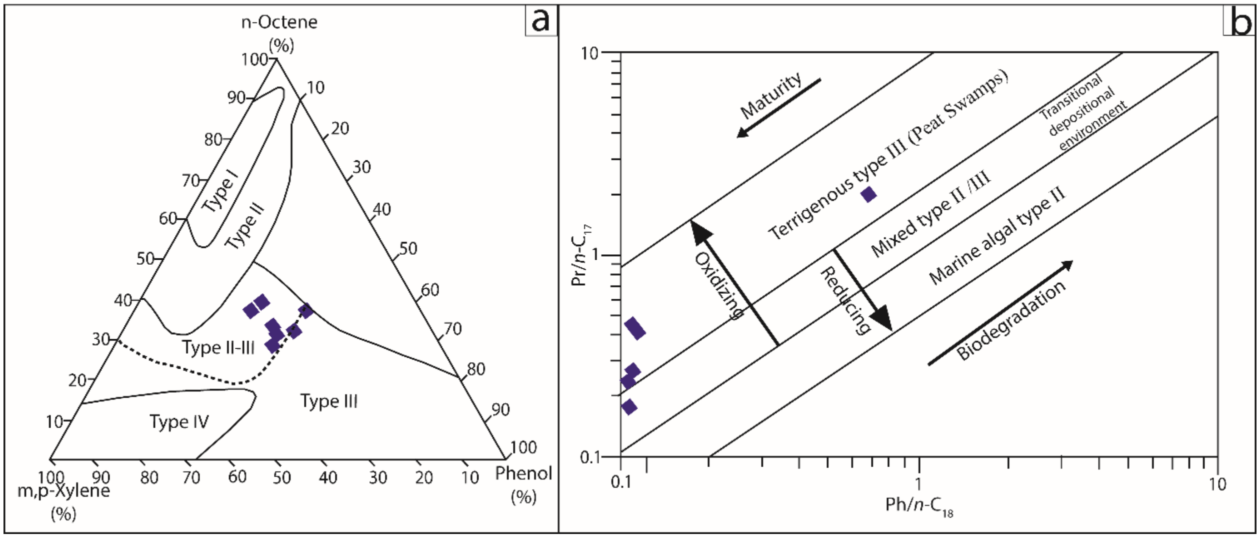

Figure 5. (b) Pr/n-$C_{17}$ versus Ph/n-$C_{18}$ plot represents the kerogen type and depositional environment of studied samples (modified after [41]). (a) Calculated parameters from Py-GC (S2) to identify kerogen type (modified after [40-41])

Table 4. Calculated parameters from kerogen pyrolysis (PY-GC)

| Sample ID | Percentage % | | |
|---|---|---|---|
| | m,p- xylene | phenol | n-octane |
| LCDC A21 | 30.76 | 34.61 | 34.61 |
| LCDC A33 | 37.31 | 31.34 | 31.34 |
| LCDC B4A | 26.38 | 34.35 | 39.26 |
| LCDC B27 | 36.22 | 33.07 | 30.70 |
| LCDC B31 | 37.77 | 24.44 | 37.77 |
| LCDC B39 | 33.52 | 36.99 | 29.47 |
| LCDC B63 | 35.10 | 26.59 | 38.29 |

Table 5. Parameters of n-alkane calculated from ion m/z 85 of the studied samples

| Sample ID | Normal Alkanes and isopronoid ion m/z 85 | | | |
|---|---|---|---|---|
| | Pr/Ph | Pr/n-$C_{17}$ | Ph/n-$C_{18}$ | CPI |
| LCDC A21 | 1.62 | 0.39 | 0.18 | 1.08 |
| LCDC A33 | 1.47 | 0.21 | 0.13 | 1.2 |
| LCDC B4A | 2.41 | 0.44 | 0.16 | 1.21 |
| LCDC B27 | 1.81 | 0.55 | 0.29 | 1.12 |
| LCDC B31 | 2.15 | 1.8 | 0.88 | 2.38 |
| LCDC B63 | 1.46 | 0.16 | 0.11 | 1 |
| LCDC B39 | 1.58 | 0.27 | 0.17 | 1.54 |

*Pr: pristane; Ph: phytane.*
*CPI: Carbon Preference Index:* $(2[n\text{-}C_{23}+n\text{-}C_{25}+n\text{-}C_{27}+n\text{-}C_{29}]/[n\text{-}C_{22}+2\{n\text{-}C_{24}+n\text{-}C_{26}+n\text{-}C_{28}\}+n\text{-}C_{30}])$.

### 4.5.2. Triterpanes (m/z 191)

The distribution of triterpanes are characterized by the m/z 191 ion chromatogram Fig. 4 of saturated hydrocarbon fraction. Labelled peaks are as listed in Table 9, and derived parameters are in Table 6. In m/z 191 mass chromatograms, the distribution shows that the Lakhra coal samples are abundant in triterpanes. High abundance of $C_{29}$ hopanes are generally observed in all studied samples. Among the hopane homologs, the dominancy of $C_{31}$ and the presence of low abundance of homohopane $C_{32}$ is the indication of sub-oxic environment, which is also supported by the absence of $C_{35}$ in the homohopanes series [49-50].

Table 6. Parameters of triterpanes and terpanes calculated from m/z 191 fingerprints of the studied samples

| | Triterpanes and terpanes (m/z191) | | | |
|---|---|---|---|---|
| Sample ID | Ts/(Ts+tm) | Tm/Ts | OI/C30 | $C_{32}$ homohopane (22S+22R) |
| LCDC A21 | 0.04 | 21.5 | 0.03 | 0.33 |
| LCDC A33 | 0.12 | 7.33 | 0.05 | 0.4 |
| LCDC B4A | 0.03 | 29.5 | - | 0.2 |
| LCDC B27 | 0.02 | 35 | 0.03 | 0.3 |
| LCDC B31 | 0.05 | 18.5 | 0.03 | 0.33 |
| LCDC B63 | 0.11 | 8 | 0.05 | 0.41 |
| LCDC B39 | 0.07 | 12.33 | 0.10 | 0.47 |

*Ts: (C27 18α (H)-22,29,30-trisnorneohopane); Tm: (C27 17α (H)-22,29,30-trisnorhopane);.*
*OI/C30: oleanane/C30 hopane*

The Tm ($C_{27}$ 17 α(H)-22,29,30-trisnorhopane) is dominated over Ts ($C_{27}$ 18α(H)-22,29,30-trisnorneohopane) with Tm/Ts ratio ranging from 8-29 which suggest dominant presence of higher plants [15]. Ts/(Ts+Tm) for the studied samples ranges from 0.032 to 0.12. Ts/(Ts+Tm) is generally a ratio to identify maturity but [52] noted that Ts/(Ts+Tm) it is not always sensitive for quantitative measurement. In the studied samples oleanane is present Fig. 6a which is a strong indicator of occurrence of terrestrial angiosperm plant input in coals of late Cretaceous or younger age [53] The presence of oleanane indicates that the organic matter were effected by marine influence [36]. Moreover for the calculated ratio of $C_{32}$ 22S/(22R + 22S), according to [54], if $C_{32}$ 22S/(22S + 22R) homohopane ratio is within <0.3 to 0.5 and with equilibrium of $C_{29}$ 20S/(20S + 20R) sterane ranges within 0.1 to 0.3 these are considered as thermally immature [55].

### 4.5.3. Steranes and diasterane (m/z 217)

The distribution of steranes and the diasteranes ($C_{27}$, $C_{28}$ and $C_{29}$) are characterized by the m/z 217 ion chromatograms Fig. 6. Peak labels are listed as in Table 9 and the derived parameters are listed in Table 7. In the m/z 217 mass chromatogram, the regular steranes are dominated by $C_{29}$ isomers which affirmed that the organic matter input are terrestrially-derived which is closely related to vascular plants [55–57]. The percentage of $C_{27}$, $C_{28}$, and $C_{29}$ steranes of the samples are in the range of 4.9 to 17.2, 15.6 to 60.0, and 32 to 72.1 respectively. The sterane abundance are in the following order: $C_{29} > C_{28} > C_{27}$ and the values are plotted on a ternary diagram of Fig. 7b which indicate the coals, as expected, are derived from higher plants of terrestrial origin. Moreover, this is also supported by the plot of pristane/phytane versus $C_{29}/C_{27}$ plot Fig. 7c as was previously reported by [37,59–61] indicating the type of organic matter is derived from land pants. The plots of $C_{29}$ 20S/(20S+20R) and $C_{29}$ $\beta\beta/(\beta\beta+\alpha\alpha)$ Fig. 17a and Tm/Ts versus $C_{29}$ 20S/(20S+20R) Fig. 7a and 9d indicate thermal maturity which is strongly in agreement with other results that support thermal immaturity of the analyzed samples.

Table 7. Parameters of steranes calculated from ion m/z 217

| | | | | | Regular steranes | | |
|---|---|---|---|---|---|---|---|
| Sample Id | $C_{29}$ 20S /(20S+20R) | $C_{29}$ $\beta\beta$ $/(\beta\beta+\alpha\alpha)$ | $C_{29}$ $/C_{27}$ | $C_{27}$ $/C_{29}$ | $C_{27}$% | $C_{28}$% | $C_{29}$% |
| LCDC A21 | 0.08 | 0.33 | 5.75 | 0.1 | 12.5 | 15.6 | 71.8 |
| LCDC A33 | 0.2 | 0.30 | 3.2 | 0.3 | 17.2 | 27.5 | 55.1 |
| LCDC B4A | 0.06 | 0.25 | 4.7 | 0.2 | 14.7 | 16.1 | 69.1 |
| LCDC B27 | 0.10 | 0.41 | 14.6 | 0.06 | 4.9 | 22.9 | 72.1 |
| LCDC B31 | 0.11 | 0.26 | 3.7 | 0.2 | 16 | 24 | 60 |
| LCDC B63 | 0.2 | 0.45 | 3.3 | 0.3 | 12 | 48 | 40 |
| LCDC B39 | 0.15 | 0.29 | 4 | 0.25 | 8 | 60 | 32 |

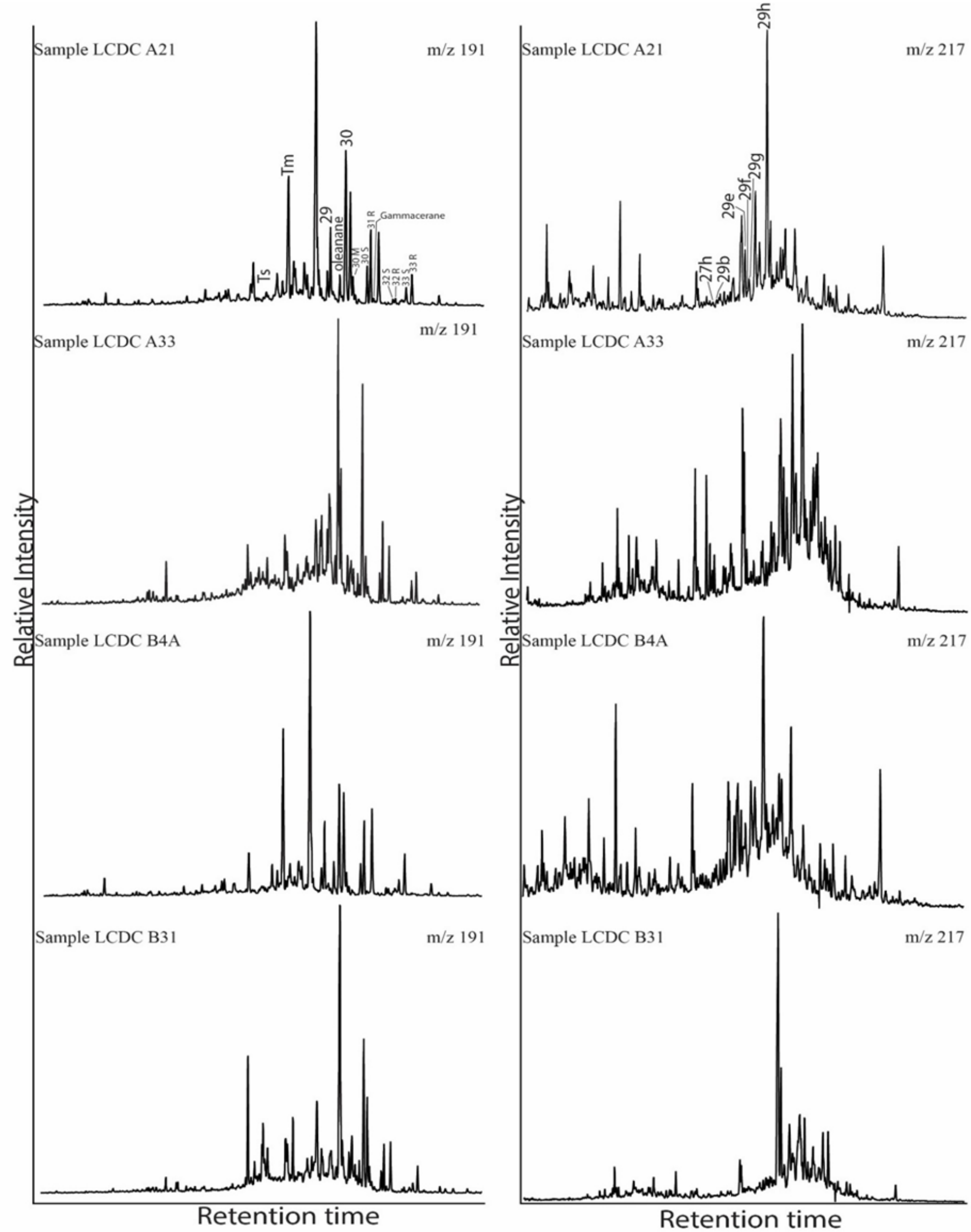

Figure 6. (a) Triterpanes interpreted traces from ion m/z 191 and, (b) Sterane and diasterane traces from ion m/z 217 for LCDC A21, LCDC A33, LCDC B4A and LCDC B31 coal samples

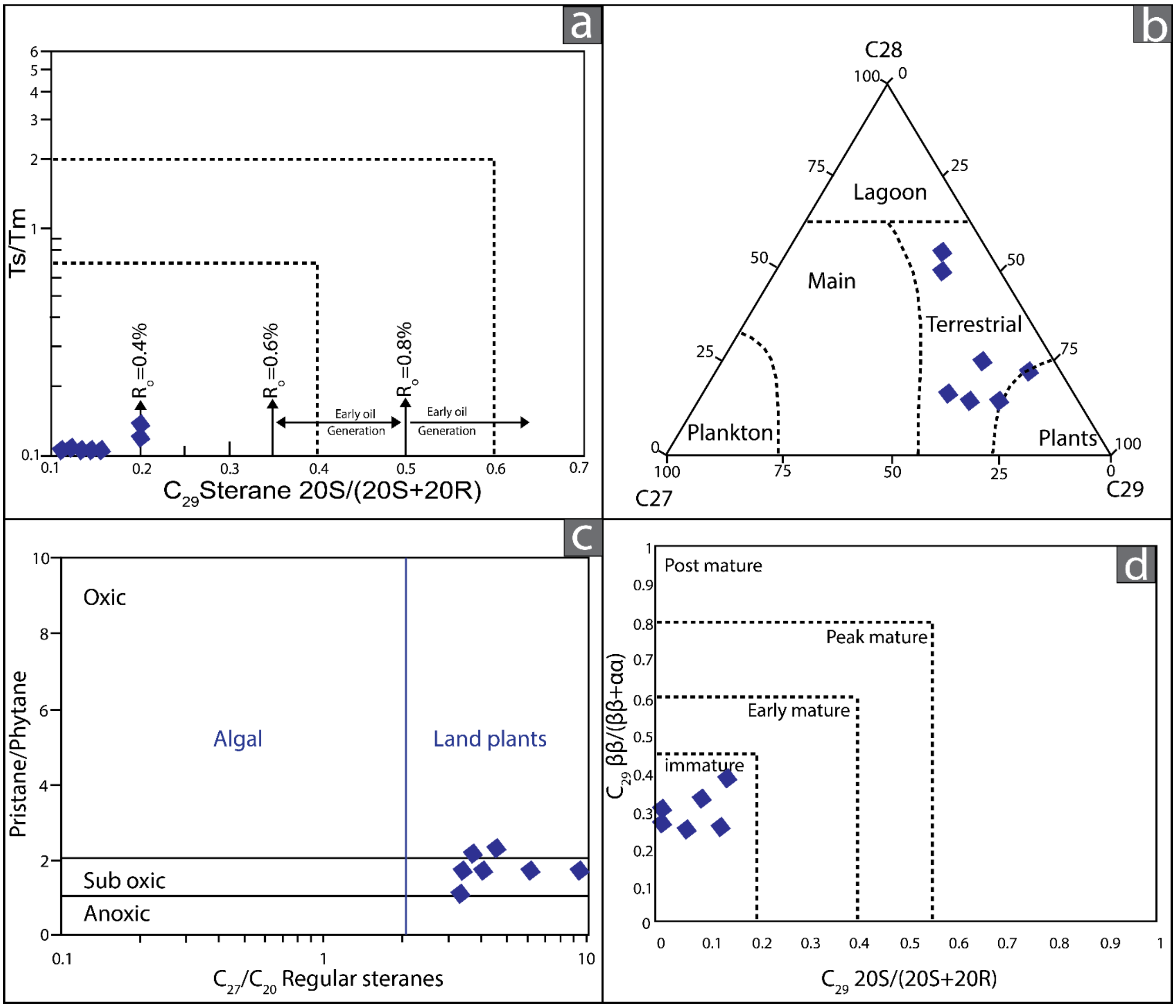

Figure 7. (a) Ts/Tm versus C29 20S/(20S+20R) and (d) C29 ββ/(ββ+αα) versus C29 20S/(20S+20R) cross plot showing low maturity of the studied samples (modified after Peters et al., 2005 [50]). (b) the ternary plot representing the dominancy of terrestrial drive organic matter deposits based on steranes distribution (after [52]) and (c), Pristane/Phytane versus C29 / C27 indicates the type of organic matter (after [38]).

## 4.6. Organic petrographic analysis

### *4.6.1. Huminite reflectance*

The reflectance measurements of huminite (ulminite and detrohuminite) are given in Table 8. The measured mean random reflectance of these studied coals varied from 0.26 to 0.32%, indicating the immature nature of the analyzed samples.

### *4.6.2. Maceral composition*

The maceral content of the analyzed coals is presented in Table 8 and examples of macerals present in the studied samples are as shown in Fig. 8. The coal samples are classified as humic coal Fig. 9a and dominated by huminite (82- 92%) with moderate amount of liptinite (5 – 14%), and low amount of inertinite (3 - 4%). TPI and GI values were calculated to indicate depositional environment and plotted on a diagram Fig. 9b that was modified after [62].

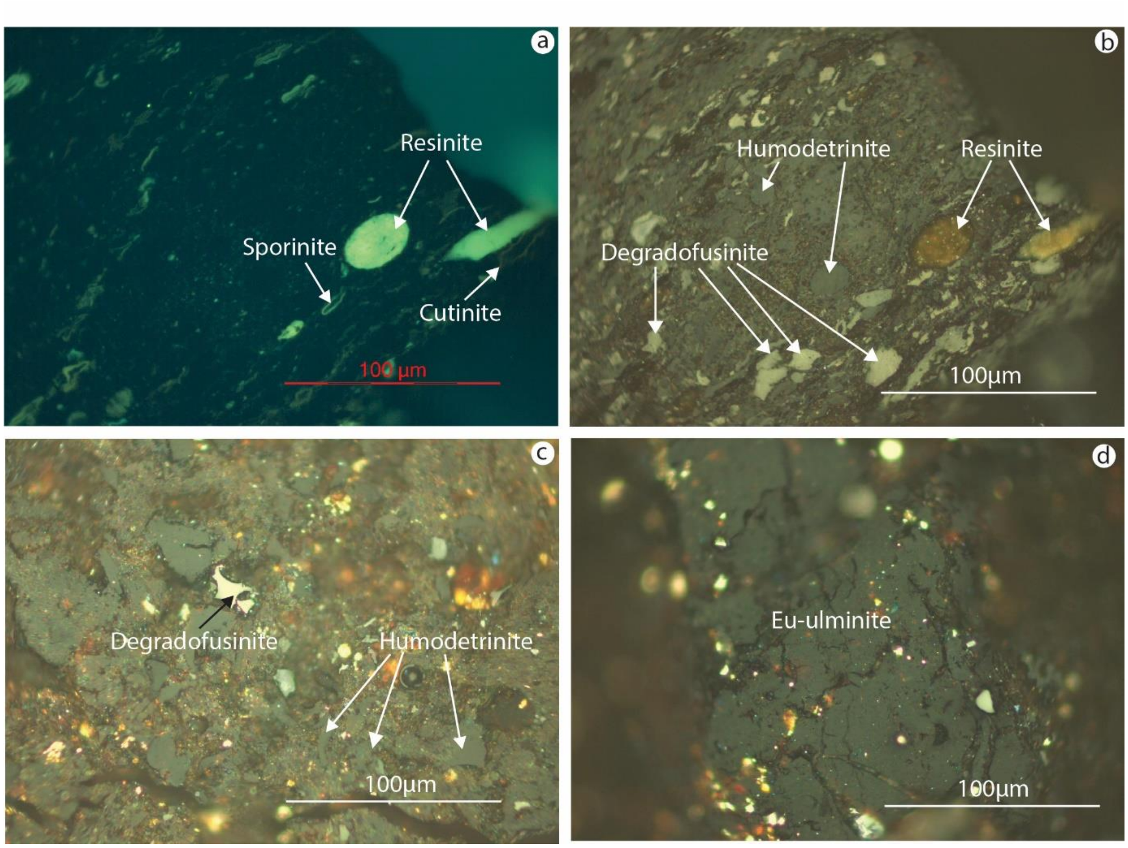

Figure 8. photomicrographs of organic matter assemblages from Bara formation coal samples of Lakhra area as shown under reflected light (b,c,d) and UV light (a) field width = 100 µm. fig (a) showing macerals from liptinite group Resinite, Sporinite and cutinite, (b) showing humodetrinite, resinite and degradofusinite, (c) showing degradofusinite and humodetrinite and, (d) showing eu-ulminite maceral

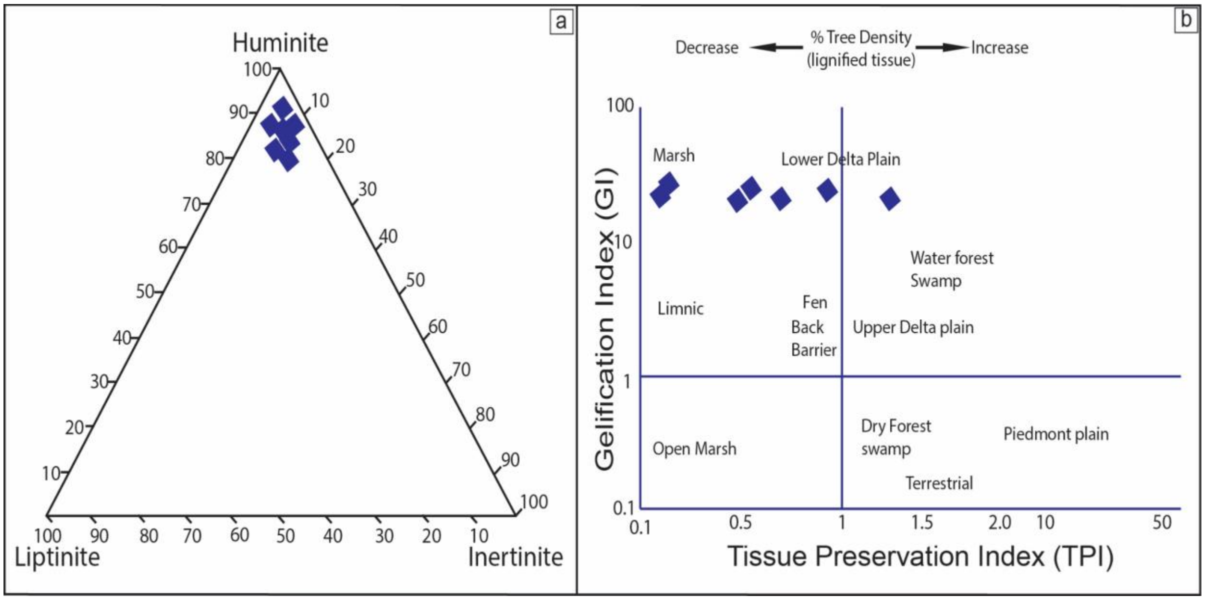

Figure 9. (a) Ternary diagram of maceral group composition (huminite, liptinite, and inertinite) for the analysed Lakhra coals. (b) Diagram of GI versus TPI indicating the paleo depositional environment of the analyzed Lakhra coals modified after (after [58])

Table 8. Huminite reflectance and maceral composition of the analysed Lakhra coals

| Sample ID | Ro% | Huminite % |  |  |  |  | Liptinite % |  |  |  |  | Inertinite % |  |  |  |  | TPI | GI |
|---|---|---|---|---|---|---|---|---|---|---|---|---|---|---|---|---|---|---|
|  |  | Tx | U | Dh | Txu | Total | Sp | Cu | Rs | Ld | Total | df | Sfu | idt | Fg | Total |  |  |
| LCDC A21 | 0.27 | 0 | 40 | 46 | 0 | 86 | 3 | 2 | 4 | 1 | 10 | 1 | 2 | 0 | 1 | 4 | 0.91 | 21 |
| LCDC A33 | 0.28 | 0 | 26 | 56 | 0 | 82 | 4 | 3 | 4 | 3 | 14 | 1 | 1 | 1 | 1 | 4 | 0.47 | 20.5 |
| LCDC B4A | 0.32 | 1 | 33 | 57 | 0 | 92 | 2 | 1 | 2 | 0 | 5 | 1 | 2 | 0 | 0 | 3 | 0.59 | 30.6 |
| LCDC B27 | 0.29 | 0 | 52 | 33 | 1 | 86 | 0 | 3 | 4 | 3 | 10 | 1 | 2 | 0 | 1 | 4 | 0.15 | 21.5 |
| LCDC B31 | 0.31 | 0 | 45 | 36 | 2 | 83 | 5 | 4 | 3 | 0 | 12 | 2 | 2 | 0 | 1 | 5 | 1.25 | 16.6 |
| LCDC B39 | 0.26 | 1 | 37 | 49 | 0 | 87 | 1 | 3 | 3 | 1 | 8 | 1 | 2 | 1 | 1 | 5 | 0.76 | 17.4 |
| LCDC B63 | 0.32 | 11 | 3 | 72 | 2 | 88 | 3 | 2 | 4 | 0 | 9 | 1 | 1 | 0 | 1 | 3 | 0.19 | 29.3 |
| Total avg % | 0.29 | 1.85 | 34 | 50 | 0.71 | 86 | 3 | 3 | 4 | 1 | 10 | 1 | 2 | 1 | 1 | 4 | 0.61 | 22.4 |

*R%: Huminite;*  
*Huminite – Tx: textininte; U: ulminite; Dh: Detrohuminite; Txu: textoulminite;*  
*Liptinite – Sp: Sporinite; Cu; Cutinite; Rs: Resinite; Ld: Liptodetrinite;*  
*Inertinite – df: degradofusinite; Sfu: semifusinite; idt: inertodetrinite; Fg: funginite;*  
*TPI: tissue preservation index; = (telohuminite+semifusinite)/(detrohuminite + macrinite + inertodetrinite);*  
*GI: Gelification index; = huminite/inertinite.*

**a) Huminite group:**

Huminite group is the most abundant macerals in the studied coals and ranging from 82 – 92% Table 8. The most abundant maceral being ulminite and detrohuminite. In huminite group, generally ulminite/textinite are known as telohuminite. Meanwhile in the studied coal samples telohuminite and detrohuminite were dominant in huminite group, which indicated the degree of degradation and decomposition of the original peat material [63]. Detrohuminite ranges from 33 to 72% with average around 50% whilst ulminite ranges from 3 to 72%. Textinite occurrence is low in 2 samples (LCDC B4A and LCDC B39) but rather common in sample LCDC B63, whilst it is not present in other samples Table 8.

**b) Liptinite group:**

The analyzed samples contain significant amount of terrestrial derived liptinite macerals that range from 5 to 14 % with an average of 10% Table 8. The liptinite macerals were identified by their nature of fluorescence in ultraviolet (UV) light. The common liptinite macerals in these coals are sporinite, cutinite, resinite, and liptodetrinite. Resinite is most common and shows yellowish-green fluorescence under UV light Fig. 8a. In reflected "white" light resinite appears as dark gray granular bodies and sometimes it occurs as cell filling in ulminite Fig 8b. Sporinite also shows yellowish-green fluorescence under UV light excitation and is commonly associated with cutinite which fluoresces less intense Fig. 8a. This intense green fluorescence collaborates with the low huminite reflectance data, therefore in support of the thermally immature nature of these organic matters.

**c) Inertinite group:**

The analysed coal samples from Lakhra coal field also contain inertinite macerals, although low in relative abundance (3 to 5%; Table 8). Identified inertinite macerals include degradefusinite, semifusinite, inertodetrinite and funginite Fig. 8c. Macrinite was also present but rare in occurrence (<1% in the studied coals). The presence of funginite suggests some influence of degradation during deposition of the plant materials that eventually formed these coals.

## 5. Discussion

### 5.1. Quality of organic matter

In this study, the type of organic matter was interpreted based on parameters that were obtained by means of organic geochemical and petrological methods. The main parameter used is HI index. According to [27], HI of between 200 to 350 is considered as Type II/III kerogen. The studied coals average HI value is 340, thus they can be considered as Type II/III kerogen. This is interpreted based on the HI versus $T_{max}$ and HI versus OI plots Fig. 3 a & b, which indicates that the organic matter within the studied sample is predominantly of Type II/III Kerogen. This is also in agreement with the results of pyrolysis-GC analyses as shown in the ternary diagram of Fig. 7b, which indicate that the analyzed coal samples are of a mixture of Type II and III kerogens. The plot of Pr/n-$C_{17}$ versus Ph/n-$C_{18}$ Fig. 5b that was modified by [46] also indicates that the organic matter is of Type II/III kerogen that was deposited in a terrigenous depositional setting.

### 5.2. Hydrocarbon generation potential

To interpret the hydrocarbon generation potential, the classification by [55] is adopted here. The results obtained from the extracted bitumen, and yielded hydrocarbons Table 2 and Fig. 2a show that the coals have excellent generation potential, and this also agrees with the Rock -Eval parameters. The average TOC values for the Lakhra coals is 53 wt%, the average for $S_2$ is 180.75 and average for $S_1$ is 3.59 mgHC/g of rock whereby the values of these parameters indicate that the analyzed coals possess excellent hydrocarbon generation potentials. The plot of Fig. 3 c & d further corroborated that the studied coals have excellent hydrocarbon generation potential, and that they can generate significantly more gas with minor oil upon maturation.

### 5.3. Thermal maturity

The thermal maturity of the Lakhra coal field samples was assessed based on parameters obtained from huminite reflectance, proximate analysis, pyrolysis data and biomarker ratios.

Huminite reflectance (%Ro) of these Lakhra samples range from 0.26% to 0.32% Table 8 indicating that the coalification degree of the analyzed Lakhra coals is of lignite to sub-bituminous C rank.

The results of the proximate geochemical analysis that was carried were compared to the classification based on the ASTM [10]. The volatile matter and fixed carbon content gave higher values, which ranges from 35.44-53.07 and 26.17-47.32 Table 1. These results of the proximate analysis is in agreement with huminite reflectance of these coals i.e. lignite or transitional to sub-bituminous C coal according to ASTM classification by [64].

Production Index (S1/S1+S2) values of the analysed coal samples are 0.02 Table 3. Values of the production index that are less than 0.1 and $T_{max}$ values less than 435°C both indicate thermally immature organic matter [65]. $T_{max}$ values of the Lakhra coals are in the range of 403-429°C, thus they are all immature. To further illustrate the maturity and kerogen type of the organic matter, an HI-Tmax diagram was plotted Fig. 3a which displayed a distribution of mixed Type III and Type II/III kerogen that falls within immature zone. $T_{max}$ values are known to vary with maturity and kerogen type of organic matter [66], although in this case no distinct variation in maturity been displayed.

In immature coals, the dominance of long-chain n-alkanes compared with short-chain n-alkanes, are attributed to terrestrial plants in higher altitudes [63-64]. The CPI values calculated from the analyzed Lakhra coal samples range from 1 to 2.38, with most values being significantly greater than 1 thus also indicate the coals are immature Table 5. Based on GC-MS fingerprints of these Lakhra coal samples, the biomarker parameters lend further support to the immature nature of the analyzed coals. As a consequence of temperature and time of thermal reactions, some biomarkers were transformed. For example, Ts (18a(H)- 22,29,30-Trisnorneohopane) is known to be more stable than Tm (17a(H)-22,29,30-Trisnorhopane) thus, the Ts/(Ts+Tm) ratio has been used as an indicator for maturity [62,65]. The Ts/(Ts+Tm) ratio calculated in this study ranges from 0.003 to 0.12, which further implies immature nature of the organic matter. The ratio of 22S/(22S+22R) for $C_{32}$ are between 0.2 – 0.47 Table 8, also suggesting that the analyzed samples are immature. Based on the m/z 217 mass fragmentogram, the 20S/(20S+20R) sterane and ββ/ (ββ+ αα) sterane ratios were determined to be 0.06 to 0.2 and 0.25 to 0.45 respectively. According to [54], if the value of 20S/(20S+20R) is equilibrium with values of ββ/(ββ+ αα) which is in between the range of 0.005 – 0.2 to 0.2 – 4.5, it represents immaturity Fig 5b, 9d, thus in agreement with other maturity parameters.

### 5.4. Paleodepositional environment

The depositional environment during the deposition of the peat-forming communities that subsequently formed the Bara Formation coals appears to be in an oxic to sub-oxic condition.

This is as illustrated in the Pr/n$C_{17}$ versus Ph/n$C_{18}$ plot of Fig. 5b, which indicates a transitional environment and that the organic matter was mainly derived from terrigenous source dominated by Type II/III kerogen. CPI values also suggest that the analysed coals were deposited under oxic-suboxic condition and is further supported by the bimodal distribution of n-alkanes as well as by relatively low Pr/Ph ratios (1.46–2.41).

Moreover, high Tm/Ts ratio of the coals are also indicative of oxic-suboxic depositional condition [38, 56, 66-67] such as in environments within a lower delta plain or paralic settings. The presence of marine influence as indicated by the occurrence of oleanane, is an important factor in the preservation of organic matter, and thus supports a deposition within a terrestrial environment under suboxic conditions [43, 49]. Marine influence has been reported to be able to help preserve the oil potential of coaly source rocks [73]. It is most probable that marine influence may have contributed to the reasonably well-preserved nature of these Bara Formation coals and thus capable of yielding an excellent amount of extractable organic matter (EOM).

The high abundance of $C_{29}$ steranes also indicates dominant of terrestrially-derived organic matter that are possibly related to vascular plants [55–57]. The concentration of $C_{27}$, $C_{28}$, and $C_{29}$ steranes as illustrated in a ternary diagram of Fig. 7b, again, as expected, provided further support that the coals were derived from higher plants of terrestrial origin.

As was revealed in the petrographic analysis, the high amount of huminite macerals with the dominance of detrohuminite Table 8, indicates a suboxic depositional condition in peat forming mires and deposition in a waterlogged condition of a wet forest environment [74]. According to [75], detrohuminte is considered to be derived from herbaceous plants and cellulose rich wood, and from poorly preserved big woody plants.

The paleoenvironment of the coal-forming peat has also interpreted using petrographic facies based on Gelification index (GI) and tissue preservation index (TPI) as shown in Fig. 9b which in support, also indicates a deposition within a lower delta plain setting.

Table 9. Ion m/z 191 and ion m/z 217 identified peaks and abbreviation

| Peak No. | Compound | Abbreviation |
|---|---|---|
| | Ion m/z 191 | |
| Ts | 18α (H),22,29,30-trisnorneohopane | Ts |
| Tm | 17α (H),22,29,30-trisnorhopane | Tm |
| 29 | 17α,21β (H)-norhopane | C29 hop |
| Oleanane | 1817α (H)-oleanane | Oleanane |
| 31S | 17α,21β (H)-homohopane (22S) | C31 (22S) |
| 31R | 17α,21β (H)-homohopane (22R) | C31 (22R) |
| 32S | 17α,21β (H)-homohopane (22S) | C32 (22S) |
| 32S | 17α,21β (H)-homohopane (22R) | C32 (22R) |
| 33S | 17α,21β (H)-homohopane (22S) | C33 (22S) |
| 33R | 17α,21β (H)-homohopane (22R) | C33 (22R) |
| | Ion m/z 217 | |
| b | 13β,17α (H)-diasteranes20R | Diasteranes |
| e | 5α,14α (H), 17α (H)-steranes 20S | ααα20S |
| f | 5α,14β (H), 17β (H)-steranes 20R | αββ20R |
| g | 5α,14β (H), 17β (H)-steranes 20S | αββ20S |
| h | 5α,14α (H), 17α (H)-steranes 20R | ααα20R |

## 6. Conclusions

Organic petrological and geochemical analyses were performed on Lakhra coals of the Bara Formation. Coal rank and petroleum generation potential as well as paleoenvironment were determined and can be concluded as follows:

1. Based on parameters of Rock Eval, kerogen type (Py-GC) & GC-MS it is suggested that the kerogen of these Lakhra coals is of Type II/III. It can also be concluded that the samples are capable of generating significantly more gas and some oil during maturation process. This assumption is also supported by maceral composition as the coals are dominated by

huminite, with low to moderate amount of liptinite. Bitumen extraction (EOM and HC yields) data evaluated in relation to TOC content also indicate the analyzed Lakhra coals to possess fairly good-excellent hydrocarbon generation potential.

2. The thermal maturity assessment based on proximate and huminite reflectance analyses suggest that the Lakhra coals are thermally immature for hydrocarbon generation being of lignite to sub-bituminous C rank. In addition, the pyrolysis $T_{max}$ data and hydrocarbon extraction yields are also in agreement that supports the immature nature of these coals.
3. The paleoenvironmental setting was interpreted as within a lower delta plain that encouraged higher land-plant growth within wet peat swamps while the occurrence of oleanane suggests a presence of marine influence and further support deposition under predominantly sub-oxic conditions. The marine influence may have enhanced the apparent oil-prone nature of these predominantly gas-prone Bara Formation coals.

## Acknowledgement

*We are highly thankful to Mr. Lalkhan Mastoi, an ex-Managing Director of Lakhra Coal Development company (LCDC) who help to access these remote area mines, by providing their transport with their honorable staff. We cannot forget the help we received from Mr. Ashraf Malah, a Project Director in LCDC who provide his best interest throughout this fieldtrip and during the data collection from mines.*

## References

[1] Qian M, Miao X, Xu J. Green mining of coal resources harmonizing with environment. J China Coal Soc 2007; 32:1–7.
[2] Elliott MA. Chemistry of coal utilization. Second supplementary volume. John Wiley and Sons, New York, NY; 1981.
[3] Wang G, Xu Y, Ren H. Intelligent and ecological coal mining as well as clean utilization technology in China: Review and prospects. Int J Min Sci Technol 2019; 29:161–169.
[4] Levine JR. Coalification: The Evolution of Coal as Source Rock and Reservoir Rock for Oil and Gas. vol. 38. AAPG Special Volumes; 1993.
[5] Rice DD, Clayton JL, Pawlewicz MJ. Characterization of coal-derived hydrocarbons and source-rock potential of coal beds, San Juan Basin, New Mexico and Colorado, USA. Int J Coal Geol 1989; 13:597–626.
[6] Wilkins RWT, George SC. Coal as a source rock for oil: a review. Int J Coal Geol 2002; 50:317–361.
[7] Petersen HI, Andersen C, Anh PH, Bojesen-Koefoed JA, Nielsen LH, Nytoft HP, Rosenberg P, Thanh L. Petroleum potential of Oligocene lacustrine mudstones and coals at Dong Ho, Vietnam—an outcrop analogue to terrestrial source rocks in the greater Song Hong Basin. J Asian Earth Sci 2001; 19:135–154.
[8] Khokhar Q, Solangi S, Hakro A. D, Abbasi S, Brohi I, Pathan M. Lithofacies of Bara Formation at wadi sawri nala section, northern lakhi range, southern indus basin, Pakistan. Sindh Univ Res Journal-SURJ Sci Ser 2014; 46.
[9] Ghaznavi MI. An overview of coal resources of Pakistan. GSP, Pre Publ Issue Rec Vol 2002.
[10] Simon FO, Khan RA, Landis ER, Hildebrand RT. Chemical and physical characterization of mine samples from Lakhra coal field, South Sind, Pakistan. US Geological Survey; 1987.
[11] Malkani MS. A review of coal and water resources of Pakistan. J Sci Technol Dev 2012; 31:202–218.
[12] Siddiqui I, Solangi SH, Samoon MK, Agheem MH. Preliminary studies of Cleat Fractures and Matrix Porosity in Lakhra and Thar coals, Sindh, Pakistan. J Himal Earth Sci 2011; 44:25–32.
[13] Ayinla HA, Abdullah WH, Makeen YM, Abubakar MB, Jauro A, Yandoka BMS, Abidin NSZ. Petrographic and geochemical characterization of the Upper Cretaceous coal and mudstones of Gombe Formation, Gongola sub-basin, northern Benue trough Nigeria: Implication for organic matter preservation, paleodepositional environment and tectonic settings. Int J Coal Geol 2017; 180:67–82.
[14] Fowler MG, Goodarzi F, Gentzis T, Brooks PW. Hydrocarbon potential of middle and upper Devonian coals from Melville Island, Arctic Canada. Org Geochem 1991; 17:681–694.
[15] Hakimi MH, Abdullah WH, Sia S-G, Makeen YM. Organic geochemical and petrographic characteristics of Tertiary coals in the northwest Sarawak, Malaysia: implications for palaeoenvironmental conditions and hydrocarbon generation potential. Mar Pet Geol 2013; 48:31–46.
[16] Hasiah AW. Oil-generating potential of Tertiary coals and other organic-rich sediments of the Nyalau Formation, onshore Sarawak. J Asian Earth Sci 1999; 17:255–267.

[17] Williams MD. Stratigraphy of the Lower Indus Basin, West Pakistan. 5th World Petroleum Congress. World Petroleum Congress; 1959.

[18] Jones AG, Manistre BE, Oliver RL, Willson GS, Scott HS. Reconnaissance Geology of part of West Pakistan (Colombo Plan co-operative project conducted and compiled by Hunting Survey Corporation). Gov Canada, Toronto 1960.

[19] Ghani M., Harbour R., Landis E., Kebblish W. Geology and coal resources of the Lakhra coal field, Hyderabad area, Pakistan. US Gelogical Survery 1975; No. 75-553.

[20] Williams MD. 19. Stratigraphy of the Lower Indus Basin, West Pakistan. 5th World Petroleum Congress. World Petroleum Congress; 1959.

[21] Nuttall WLF. The larger foraminifera of the Upper Ranikot Series (Lower Eocene) of Sind, India. Geol Mag 1926; 63:112–121.

[22] Vredenburg EW. Nummulites douvillei, an undescribed species from Kachh with remarks on the zonal distribution of Indian Nummulites. Rec Geol Surv India 1906; 34:79–95.

[23] Vredenburg EW. A Supplement to the" Mollusca" of the Ranikot Series. Government of India Central publication branch; 1928.

[24] Espitalié J, Laporte JL, Madec M, Marquis F, Leplat P, Paulet J, Boutefeu A. Méthode rapide de caractérisation des roches mètres, de leur potentiel pétrolier et de leur degré d'évolution. Rev l'Institut Français Du Pétrole 1977; 32:23–42.

[25] Dembicki Jr H, Horsfield B, Ho TTY. Source rock evaluation by pyrolysis-gas chromatography. Am Assoc Pet Geol Bull 1983; 67:1094–1103.

[26] Dembicki Jr H. Three common source rock evaluation errors made by geologists during prospect or play appraisals. Am Assoc Pet Geol Bull 2009; 93:341–356.

[27] Peters KE, Cassa MR. Applied source rock geochemistry: Chapter 5: Part II. Essential elements 1994.

[28] Orem WH, Finkelman RB. Coal formation and geochemistry. vol. 7. 2003.

[29] Othman R. Petroleum Geology of the Gunnedah-Bowen-Surat Basins, Northern New South Wales: Stratigraphy, Organic Petrology and Organic Geochemistry 2003.

[30] Bordenave ML. Applied petroleum geochemistry. Technip Paris; 1993.

[31] Makeen YM, Abdullah WH, Hakimi MH, Elhassan OMA. Organic geochemical characteristics of the Lower Cretaceous Abu Gabra Formation in the Great Moga oilfield, Muglad Basin, Sudan: Implications for depositional environment and oil-generation potential. J African Earth Sci 2015; 103:102–112.

[32] Abbassi S, Edwards DS, George SC, Volk H, Mahlstedt N, di Primio R, Horsfield B. Petroleum potential and kinetic models for hydrocarbon generation from the Upper Cretaceous to Paleogene Latrobe Group coals and shales in the Gippsland Basin, Australia. Org Geochem 2016; 91:54–67.

[33] Eglinton TI, Damsté JSS, Kohnen MEL, de Leeuw JW. Rapid estimation of the organic sulphur content of kerogens, coals and asphaltenes by pyrolysis-gas chromatography. Fuel 1990; 69:1394–1404.

[34] Giraud A. Application of pyrolysis and gas chromatography to geochemical characterization of kerogen in sedimentary rock. Am Assoc Pet Geol Bull 1970; 54:439–455.

[35] Larter SR, Douglas AG. A pyrolysis-gas chromatographic method for kerogen typing. Phys Chem Earth 1980; 12:579–583.

[36] Alias FL, Abdullah WH, Hakimi MH, Azhar MH, Kugler RL. Organic geochemical characteristics and depositional environment of the Tertiary Tanjong Formation coals in the Pinangah area, onshore Sabah, Malaysia. Int J Coal Geol 2012; 104:9–21.

[37] Farhaduzzaman M, Abdullah WH, Islam MA. Depositional environment and hydrocarbon source potential of the Permian Gondwana coals from the Barapukuria Basin, Northwest Bangladesh. Int J Coal Geol 2012; 90:162–179.

[38] Larter SR, Senftle JT. Improved kerogen typing for petroleum source rock analysis. Nature 1985; 318:277.

[39] Abdullah WH, Togunwa OS, Makeen YM, Hakimi MH, Mustapha KA, Baharuddin MH, Sia S-G, Tongkul F. Hydrocarbon source potential of Eocene-Miocene sequence of Western Sabah, Malaysia. Mar Pet Geol 2017; 83:345–361.

[40] Grice K, Schaeffer P, Schwark L, Maxwell JR. Molecular indicators of palaeoenvironmental conditions in an immature Permian shale (Kupferschiefer, Lower Rhine Basin, north-west Germany) from free and S-bound lipids. Org Geochem 1996; 25:131–147.

[41] Zunic WM, Ding S, Durig JR, Cohen AD. Pyrolysis GC/FID/FT-IR, pyrolysis GC/MS, and FT-IR studies of pore water extracts derived from peat samples differing in depositional environments. J Mol Struct 1992; 267:371–376.

[42] Kaur S, Gill JP, Evershed RP, Eglinton G, Maxwell JR. Computerised gas chromatographic—mass spectrometric and high-performance liquid chromatographic analysis of sedimentary benzoporphyrins. J Chromatogr A 1989; 473:135–151.
[43] Traoré M, Kaal J, Cortizas AM. Potential of pyrolysis-GC–MS molecular fingerprint as a proxy of Modern Age Iberian shipwreck wood preservation. J Anal Appl Pyrolysis 2017; 126:1–13.
[44] Bray EE, Evans ED. Distribution of n-paraffins as a clue to recognition of source beds. Geochim Cosmochim Acta 1961; 22:2–15.
[45] Powell TG, McKirdy DM. Relationship between ratio of pristane to phytane, crude oil composition and geological environment in Australia. Nat Phys Sci 1973; 243:37.
[46] Tissot B, Deroo G, Hood A. Geochemical study of the Uinta Basin: formation of petroleum from the Green River formation. Geochim Cosmochim Acta 1978; 42:1469–1485.
[47] Chandra K, Mishra CS, Samanta U, Gupta A, Mehrotra KL. Correlation of different maturity parameters in the Ahmedabad-Mehsana block of the Cambay basin. Org Geochem 1994; 21:313–321.
[48] Didyk BM, Simoneit BRT, Brassell SC t, Eglinton G. Organic geochemical indicators of palaeoenvironmental conditions of sedimentation. Nature 1978; 272:216.
[49] Tissot BP, Welte DH. Diagenesis, catagenesis and metagenesis of organic matter. Petroleum Formation and Occurrence. Springer; 1984:69–73.
[50] Hunt JM. Generation of gas and oil from coal and other terrestrial organic matter. Org Geochem 1991; 17:673–680.
[51] Ramanampisoa L, Radke M, Schaeffer RG, Littke R, Rullkötter J, Horsfield B. Organic-geochemical characterisation of sediments from the Sakoa coalfield, Madagascar. Org Geochem 1990; 16:235–246.
[52] Waples DW, Machiharia T. Biomarkers for geologists 1991.
[53] Ekweozor CM, Telnaes N. Oleanane parameter: verification by quantitative study of the biomarker occurrence in sediments of the Niger delta. Org Geochem 1990; 16:401–413.
[54] El Diasty WS, Moldowan JM. The Western Desert versus Nile Delta: A comparative molecular biomarker study. Mar Pet Geol 2013; 46:319–334.
[55] Peters KE, Peters KE, Walters CC, Moldowan JM. The biomarker guide. vol. 1. Cambridge university press; 2005.
[56] Czochanska Z, Gilbert TD, Philp RP, Sheppard CM, Weston RJ, Wood TA, Woolhouse AD. Geochemical application of sterane and triterpane biomarkers to a description of oils from the Taranaki Basin in New Zealand. Org Geochem 1988; 12:123–135.
[57] Huang W-Y, Meinschein WG. Sterols as ecological indicators. Geochim Cosmochim Acta 1979; 43:739–745.
[58] Robinson KM. An overview of source rocks and oils in Indonesia 1987.
[59] Karavas FA, Riediger CL, Fowler MG, Snowdon LR. Oil families in Mannville Group reservoirs of southwestern Alberta, Western Canada sedimentary basin. Org Geochem 1998; 29:769–784.
[60] Gorter JD. A Marine Source Rock in the Gippsland Basin? 2001.
[61] Liu B, Zhang G, Mao F, Liu J, Lü M. Geochemistry and origin of Upper Cretaceous oils from the Termit Basin, Niger. J Pet Geol 2017; 40:195–207.
[62] Diessel CFK. On the correlation between coal facies and depositional environments. Proceeding 20th Symposium of Department Geology, University of New Castle, New South Wales. 1986:19–22.
[63] Hackley PC, Warwick PD, Breland Jr FC. Organic petrology and coalbed gas content, Wilcox Group (Paleocene–Eocene), northern Louisiana. Int J Coal Geol 2007; 71:54–71.
[64] Stach E. Stach’s textbook of coal petrology 1982.
[65] Merrill RK. Source and migration processes and evaluation techniques 1991.
[66] Hunt JM. Petroleum Geochemistry and Geology. W.H. Freeman; 1996.
[67] Bechtel A, Sachsenhofer RF, Markic M, Gratzer R, Lücke A, Püttmann W. Paleoenvironmental implications from biomarker and stable isotope investigations on the Pliocene Velenje lignite seam (Slovenia). Org Geochem 2003; 34:1277–1298.
[68] Wang T-G, Simoneit BRT. Organic geochemistry and coal petrology of Tertiary brown coal in the Zhoujing mine, Baise Basin, South China: 2. Biomarker assemblage and significance. Fuel 1990; 69:12–20.
[69] Seifert WK, Moldowan JM. Applications of steranes, terpanes and monoaromatics to the maturation, migration and source of crude oils. Geochim Cosmochim Acta 1978; 42:77–95.

[70] Amijaya H, Schwarzbauer J, Littke R. Organic geochemistry of the Lower Suban coal seam, South Sumatra Basin, Indonesia: palaeoecological and thermal metamorphism implications. Org Geochem 2006; 37:261–279.

[71] Peters KE, Moldowan JM. The biomarker guide: interpreting molecular fossils in petroleum and ancient sediments 1993.

[72] Murray AP, Sosrowidjojo IB, Alexander R, Kagi RI, Norgate CM, Summons RE. Oleananes in oils and sediments: evidence of marine influence during early diagenesis? Geochim Cosmochim Acta 1997; 61:1261–1276.

[73] Sykes R, Volk H, George SC, Ahmed M, Higgs KE, Johansen PE, Snowdon LR. Marine influence helps preserve the oil potential of coaly source rocks: Eocene Mangahewa Formation, Taranaki Basin, New Zealand. Org Geochem 2014; 66:140–163.

[74] Flores D. Organic facies and depositional palaeoenvironment of lignites from Rio Maior Basin (Portugal). Int J Coal Geol 2002; 48:181–195.

[75] Teichmüller M. The genesis of coal from the viewpoint of coal petrology. Int J Coal Geol 1989; 12:1–87.

*To whom correspondence should be addressed: Zain Gul, Department of Geoscience, University of Technology Petronas, Malaysia,* E-mail: *zaingulau@gmail.com*